Available online at www.sciencedirect.com
ScienceDirect
Journal of Colloid and Interface Science 308 (2007) 485–490
JOURNAL OF Colloid and Interface Science
www.elsevier.com/locate/jcis

The sponge phase of a mixed surfactant system

A. Maldonado [a,*], R. Ober [b], T. Gulik-Krzywicki [c], W. Urbach [d], D. Langevin [e]

[a] *Departamento de Física, Universidad de Sonora, Apdo. Postal 1626, 83000 Hermosillo, Sonora, Mexico*
[b] *Laboratoire de Physique de la Matière Condensée, URA 792 CNRS, Collège de France, 11, Place Marcelin Berthelot, 75231 Paris Cedex, France*
[c] *Centre de Génétique Moléculaire, CNRS, 91198 Gif-sur-Yvette, France*
[d] *Laboratoire de Physique Statistique, URA 1302 CNRS, Ecole Normale Supérieure, 24, rue Lhomond, 75231 Paris Cedex, France*
[e] *Laboratoire de Physique des Solides, UMR 8502, Université Paris-Sud, Bât. 510, 91405 Orsay Cedex, France*

Received 29 May 2006; accepted 6 January 2007
Available online 11 January 2007

Abstract

We study the sponge phase of the mixed non-ionic/ionic surfactant system C_{14}DMAO–TTAB–hexanol–brine. Our aim is to determine if this phase exists in this mixed system and if it preserves or changes its structure when the relative amount of the charged surfactant is increased in the mixture. SAXS, FFEM, and conductivity results show that for the same bilayer volume fraction the sponge phase preserves its global structure. We propose a method to determine the geometrical obstruction factor from electrical conductivity measurements in ionic sponge phases. Analysis of lamellar phases in the same system shows that the bilayer thickness increases when the ionic surfactant concentration is increased.

Keywords: Surfactant; Sponge phase; Lamellar phase; SAXS; FFEM; Electrical conductivity

1. Introduction

Surfactant bilayer phases provide model systems for the study of membranes [1]. Among these phases, the lamellar and sponge phases are stable in a number of surfactant systems [2–5]. Their structure has been very well characterized by small-angle X-ray scattering (SAXS), small-angle neutron scattering (SANS) as well as by freeze-fracture electron microscopy (FFEM).

The lamellar phase (or L_α) is a regular stack of surfactant bilayers with periodicity d; it is birefringent with a high viscosity. On the other hand, the sponge phase is a disordered and infinitely connected array of bilayers. It is also called L_3 phase or disordered lamellar structure [6]. Its structure is similar to that of a bicontinuous phase. It can be pictured as a melted cubic phase, where the passages divide space in two independent regions [7]. Macroscopically, it presents some interesting properties such as a very low viscosity and flow birefringence. The topology of sponge phases, as well as that of bicontinuous microemulsions, can vary from symmetric (same volume on both sides of membranes) to asymmetric (connected infinite bilayers coexisting with vesicles). Symmetric phases are characterized by zero mean curvature at the mid-surface of the bilayer, so that both constituent monolayers are curved equally; asymmetric phases have nonzero mean curvature at the mid-surface of the bilayer [8]. Scattering experiments can be used in order to determine the topology of sponge phases and bicontinuous microemulsions [9–11].

Generally, lamellar and sponge phases are found in neighboring phase diagram regions. For many systems, both phases are stable over a large range of surfactant concentrations [2–5]. Simple binary mixtures of non-ionic ($C_{12}E_5$) [3] or ionic surfactants (AOT) [2] in water or brine display both phases. In mixtures with more components, a cosurfactant is added in order to stabilize them. This is the case of the ternary systems CPCl (ionic)–hexanol–brine [4] and C_{14}DMAO (zwitterionic)–hexanol–water [5]. All these systems show similar trends in their phase diagrams. The variation of one parameter (temperature, salt or cosurfactant concentration) induces almost the same phase sequence in most of them.

Bilayer phases can also exist in more complicated systems. For instance, the mixture of ionic and non-ionic surfactants.

* Corresponding author.
E-mail address: maldona@fisica.uson.mx (A. Maldonado).

0021-9797/$ – see front matter © 2007 Published by Elsevier Inc.
doi:10.1016/j.jcis.2007.01.012

Hoffmann and co-workers have shown that C_{14}DMAO can be mixed with an ionic surfactant, TTAB, and that the same bilayer phases of the non-mixed system are produced with the pseudoternary system: mixed surfactant–hexanol–brine [12], at least in the dilute regime (surfactant concentration: 100 mM; surfactant volume fraction $\phi \equiv V_{\text{surfactant}}/V_{\text{sample}} \approx 0.03$).

In this work, we study the sponge phase of the mixed surfactant system C_{14}DMAO–TTAB–hexanol–brine in the more concentrated regime. We explore phases with bilayer volume fractions ϕ between 0.1 and 0.4. Our aim is to determine if the sponge phase is still present at these high concentrations in the mixed system, and if it preserves or modifies its structure as the relative amount of the charged surfactant is increased in the mixture.

2. Experimental

The surfactants used are: tetradecyldimethyl aminoxide (C_{14}DMAO) which was recrystallized twice, and tetradecyltrimethyl ammonium bromide (TTAB, 99% purity) used as received. C_{14}DMAO was a gift from Dr. H. Hoffmann. TTAB was purchased from Sigma–Aldrich (99% purity). Hexanol was used as cosurfactant. We used a 60 mM NaBr brine solution as solvent. All samples were prepared with ultra-purified water.

C_{14}DMAO is a zwitterionic surfactant the phase diagram of which displays large lamellar and sponge regions when diluted in water with a short-chain alcohol as cosurfactant [5]. A lamellar phase is obtained with a cosurfactant/surfactant mass ratio $r = 0.85$. Addition of hexanol stabilizes a sponge phase ($r = 0.9$). We prepared these phases with surfactant volume fractions in the range $0.1 \leqslant \phi \leqslant 0.4$. We shall designate the C_{14}DMAO–hexanol–water system as non-mixed. At an alkaline pH, as in our experiments, C_{14}DMAO can be considered as an essentially non-ionic surfactant.

In this work, we replaced amounts of C_{14}DMAO by the cationic surfactant TTAB. The relative concentration of the ionic surfactant in the system is defined as

$$\chi_c = \frac{[\text{TTAB}]}{[\text{surfactant}]},$$

where [TTAB] is the molar concentration of TTAB and [surfactant] the total surfactant molar concentration. We studied the whole range of relative concentrations, from the non-ionic system, $\chi_c = 0$, to the fully ionic one, $\chi_c = 1$. We designate the system [C_{14}DMAO–TTAB]–hexanol–brine as the mixed system.

The sponge and lamellar phases have been studied by small angle X-ray scattering (SAXS). We use a Rigaku rotating anode source that produces the Cu$K\alpha$ lines (1.54 Å) with a fine focus (1 mm × 0.1 mm). The output was collimated by a gold-plated quartz mirror. The linear detector, with 512 channels, was placed 81 cm from the sample position. The resolution of the direct beam was measured to be $\Delta q = 0.0017$ Å^{-1} full width at half maximum. In these experiments the collimation corrections are negligible.

Freeze-fracture electron microscopy (FFEM) has been used to directly visualize the structure of the surfactant phases. The samples were prepared with a 30% glycerol and 70% water mixture as solvent to avoid the formation of ice crystals. The liquid is squeezed between two thin metal plates and then plunged into liquid propane. A platinum–carbon replica is done after fracture of the cryofixed sample with a cooled knife.

Conductivity measurements were carried out with a Melstrohm apparatus (Model E518). Since the electrical conductivity of the non-mixed system is very low, an amount of salt (NaBr), equivalent to that used in the mixed system, has been added in order to measure the obstruction factor of the sponge phase. Using brine as solvent has no appreciable effect on the phase diagram of the non-ionic system.

3. Results and discussion

We have prepared sponge and lamellar phases by varying the TTAB to total surfactant concentration ratio, χ_c, between 0 and 1. We prepared these phases with bilayer volume fractions $\phi \equiv V_{\text{surfactant}}/V_{\text{sample}}$ between 0.1 and 0.4. When a brine solution is used as solvent we observe the same qualitative behavior as in the non-ionic system. A birefringent, high-viscosity lamellar phase can be prepared at the appropriate cosurfactant/surfactant ratio. Adding cosurfactant to the system induces the L_α to L_3 transition: the birefringence observed between crossed polarizers is lost and the viscosity decreases. For all the bilayer volume fractions, ϕ, and relative concentrations of ionic surfactant, χ_c, the sponge phases display the same macroscopic characteristics: they are transparent, isotropic and have low viscosity.

3.1. SAXS results

The SAXS spectra of the studied sponge phases display a broad Bragg peak. The general features of the spectra are the same for all the TTAB/C_{14}DMAO relative concentrations, as shown in Fig. 1 for samples of bilayer volume fraction $\phi = 0.15$. The broadness of the peaks is due to the lack of long-range order in the sponge structure. The peak position $q_{\max}$ is

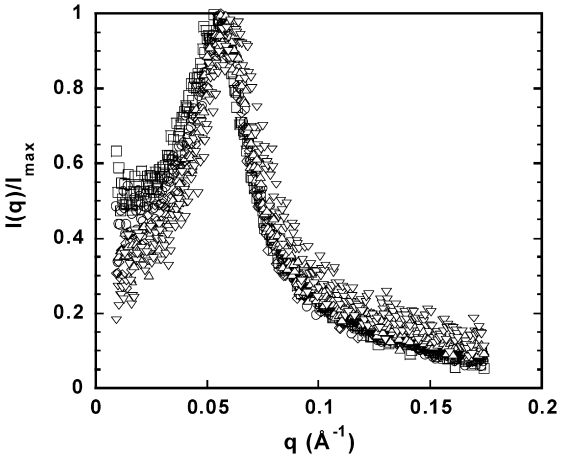

Fig. 1. SAXS spectra of sponge phases with same bilayer volume fraction, $\phi = 0.15$, but different relative concentrations of ionic surfactant: $\chi_c = 0$ (circles), 0.25 (squares), 0.5 (diamonds), 0.75 (triangles), and 1 (inverted triangles).

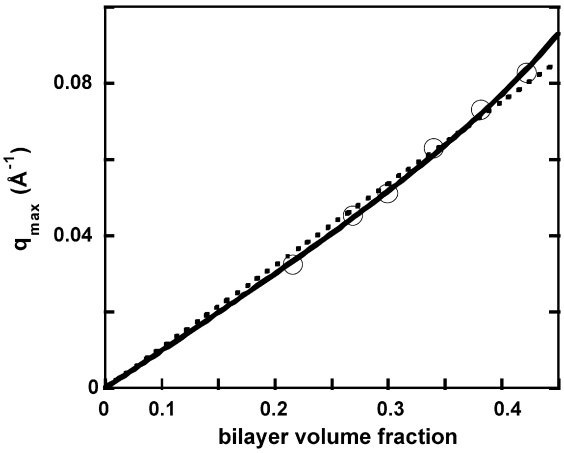

Fig. 2. Full swelling curve for the ionic sponge phase ($\chi_c = 1$). The full line is a fit to the predicted curve for symmetric sponge phases [8]. The broken line is a fit to the classical linear swelling law.

related to a characteristic distance d in the system: the mean interbilayer distance or the average passage diameter; as usual, $d = 2\pi/q_{max}$. In our system, the peaks are located at almost the same position (Fig. 1). Thus, the mean interbilayer distance does not appreciably change with different χ_c. For the samples of Fig. 1, this interbilayer distance is 110 Å.

The peak position in the scattering spectra is related to the bilayer volume fraction ϕ by the classical swelling law

$$q_{max} = \alpha \frac{2\pi}{\delta}\phi, \tag{1}$$

where δ is the bilayer thickness and α a geometrical factor whose value is in the range 1.4–1.6 [4,13–15]. With these values we can predict a bilayer thickness in the range 23 Å $< \delta <$ 27 Å for the samples of Fig. 1. This prediction can be compared with the values obtained from SAXS experiments in lamellar phases.

Note that sponge phases can have a symmetric (same volume on both sides of membranes) or asymmetric (connected infinite bilayers coexisting with vesicles) topology [8]. The scattering spectra of both type of phases are difficult to discriminate [16]. However, a plot of scattering data as a function of composition allows identification of symmetric and asymmetric structures [8]. The form of the swelling curve, i.e., a plot of the Bragg peak position, q_{max} (or the related mean interbilayer distance d), versus bilayer volume fraction ϕ, has been used in order to show that the sponge phase of the C_{14}DMAO–hexanol–water system [11], as well as that of the mixture sodium dodecyl sulfate (SDS)–pentanol–brine is symmetric [8]. On the other hand, the same kind of experiments have shown that the sponge phases of the systems water–dodecane–pentanol–SDS [8] and DDAB–tetradecane–water [9] are asymmetric. In order to assess what kind of topology we have in the ionic system, in Fig. 2 we plot the full swelling curve for $\chi_c = 1$. In the same figure we show a fit to the classical swelling law represented by Eq. (1) (broken line). We see that the fit is acceptable but departures can be observed in all the curve. In the same figure, we plot a fit to the curve predicted for symmetric structures by Engblom and Hyde [8]. The fit is very good, meaning that the sponge phases

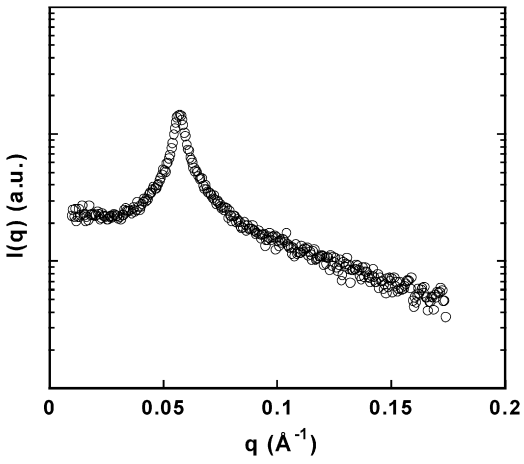

(a)

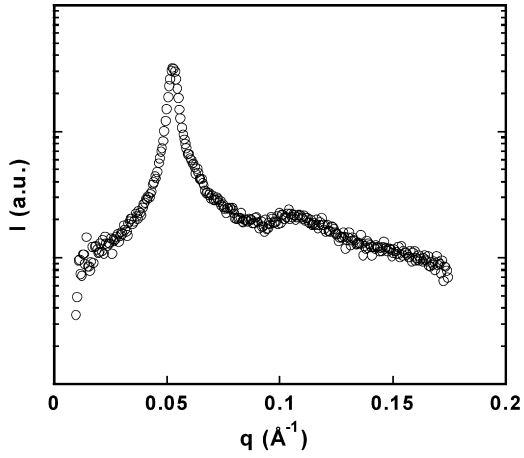

(b)

Fig. 3. SAXS spectra of lamellar phases with the same bilayer volume fraction ($\phi = 0.2$), but different composition of ionic–non-ionic surfactant. (a) $\chi_c = 0.25$ and (b) $\chi_c = 1$. Note the appearance of a second Bragg peak in the fully ionic system (b). The vertical axis is in a logarithmic scale.

are of symmetrical topology. A similar result has been obtained previously for the non-ionic system [11].

In the phase diagram, the sponge phase is located in the vicinity of a lamellar phase. For all surfactant volume fractions, the difference between both phases is a slightly different co-surfactant/surfactant ratio. It is reasonable to assume that both phases are composed of the same bilayers, oriented in a different way. Thus, one can obtain information about these bilayers by performing SAXS experiments in lamellar phases. All the scattering spectra of the L_α phases (Fig. 3) display a well-defined Bragg peak, related to the mean interbilayer distance by the Bragg equation: $d = 2\pi/q_{max}$.

We obtained the bilayer thickness by following the swelling law of the lamellar phases, which relates d to the bilayer volume fraction ϕ. If one considers flat bilayers of thickness δ, the classical swelling law is obtained: $d = \delta/\phi$ [1]. In our system, these phases can be prepared within a very large range of surfactant concentrations, allowing the swelling of the system from interlamellar distances of the order of 100 to 1000 Å. In all cases, we observed the classical linear behavior, in agreement with previous results obtained for the non-ionic system [11]. We

computed the swelling laws for lamellar phases with $\chi_c = 0$, 0.25, 0.5, 0.75, and 1, and surfactant volume fractions between $\phi = 0.2$ and $\phi = 0.4$. From the theoretical fits we have extracted the bilayer thickness δ. The bilayer thickness changes only slightly with χ_c. This parameter lies within 23.8 ± 0.5 and 25.4 ± 0.2 when χ_c varies from 0 to 1. We see that these δ values are in good agreement with the expected values for sponge phases (Eq. (1)).

One interesting behavior of the SAXS spectra of lamellar phases is that for a fixed surfactant volume fraction, the higher is χ_c, the sharper is the Bragg peak. This effect indicates that the bilayer stiffens when the ionic surfactant replaces the non-ionic one. This conclusion is reinforced by the fact that with the higher TTAB contents, the second-order Bragg peak is observed in the SAXS spectra (Fig. 3b). This second-order peak is hidden in the non-ionic samples because of thermal fluctuations.

3.2. FFEM results

The narrow peaks observed in the scattering spectra for the lamellar phases show unambiguously that they are formed by a regular stack of bilayers for all χ_c. In the case of the sponge phase, we have to be more cautious before concluding that we have the same structure for all χ_c. In fact, several lyotropic structures can generate broad correlation scattering peaks, and complementary experiments are needed in order to determine the structure of the phases.

FFEM is a technique used frequently to discriminate between possible structures in lyotropic systems. Hoffmann et al. have used it extensively in the case of the non-ionic system ($\chi_c = 0$) [5] and in the non-screened mixed system [12], where the sponge phase is unstable. In this work, we have taken freeze-fracture micrographs of sponge phases for $\chi_c \neq 0$. In all samples the solvent was a 60 mM brine solution.

In Fig. 4, we present a FFEM picture of a sponge phase with bilayer volume fraction, $\phi = 0.15$, and $\chi_c = 0.65$. The FFEM photograph reveals a typical sponge structure for both values of χ_c. No coexistence with vesicles has been observed, meaning that the sponge phase is of symmetric topology, in agreement with the SAXS results. A similar result is observed for all the ionic surfactant concentrations, even when C_{14}DMAO is replaced completely by the ionic surfactant TTAB ($\chi_c = 1$). The FFEM observations, together with the SAXS results, indicate that it is possible to obtain similar sponge phases with different ionic surfactant amounts when the solvent is a brine solution.

3.3. Electrical conductivity results

Electrical conductivity experiments can give some insight into the local geometry of the bilayer structure of the sponge phase. Ion mobility is hindered by the bilayer network and thus electrical conductivity depends on the local topology. The obstruction factor f of an sponge phase, defined as

$$f \equiv \frac{\sigma}{\sigma_0(1-\phi)}, \tag{2}$$

decreases linearly with the surfactant volume fraction ϕ [4]. In this equation, σ, the conductivity of the L_3 phase, is normalized by σ_0, the conductivity of the solvent. The factor $(1-\phi)$ takes into account the fact that the effective volume for ion movement is the solvent volume. In the case of the sponge phase, the value of f for increasingly small surfactant volume fractions ($\phi \to 0$) tends to 0.6 for defect-free bilayers [4]. Larger values of f for $\phi \to 0$ are interpreted as evidence for the appearance of holes in the membrane.

In order to know if the bilayers are decorated with pores, we have performed electrical conductivity experiments for both the non-ionic system ($\chi_c = 0$) and the fully ionic one ($\chi_c = 1$). Samples with different values of χ_c should have an intermediate behavior between these two extreme cases.

In the first case, since in our experimental conditions (pH 8.5) C_{14}DMAO is a non-ionic surfactant, the electrical conductivity σ of the sponge phases is very low. We added an amount of salt (NaBr, 60 mM) in order to obtain measurable values of σ. The phase diagram is not modified by this addition, at least in the region we prepared our samples. In Fig. 5 we show the obstruction factor ϕ of the non-ionic sponge phase (circles) as a function of the bilayer volume fraction. We observe a linear variation as expected. The negative slope reflects

Fig. 4. FFEM picture of a sponge phase prepared with a mixture of C_{14}DMAO and TTAB ($\chi_c = 0.65$). The bilayer volume fraction is 0.15.

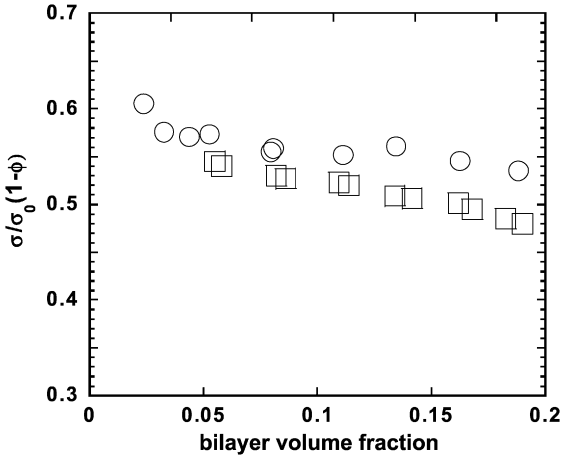

Fig. 5. Obstruction factors from conductivity measurements for the non-ionic (circles) and the ionic (squares) sponge phases.

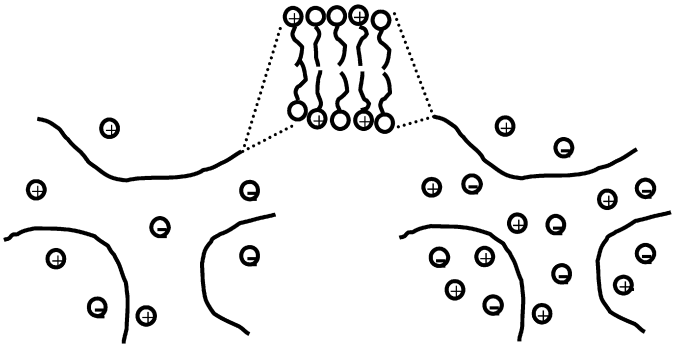

Fig. 6. Scheme of two sponge phases with same surfactant content but different salt concentrations (c_1 and c_2) in the solvent. By taking the difference in electrical conductivities between both phases ($|\sigma_1 - \sigma_2|$), the contribution of the surfactant can be eliminated and the geometrical obstruction factor can be measured.

the decrease in ion mobility due to the increase of the surfactant volume fraction, i.e., of the number of surfactant bilayers per unit volume. Furthermore, the extrapolation to $\phi \to 0$ gives a value near to 0.6 in favor of hole-free bilayers.

When we measure the electrical conductivity of the fully ionic sponge phase, $\chi_c = 1$, we must take into account the fact that the surfactant is charged. When we increase the surfactant volume fraction, we also increase the charge content (we add amphiphilic charged molecules as well as the counter-ions). Since we wanted to measure the purely geometrical obstruction factor, we performed the experiment in two steps in order to eliminate the conductivity of the ionic surfactant. We measured the electrical conductivities σ_1 and σ_2 of two sponge phases with the same surfactant content but different NaBr concentrations c_1 and c_2 (Fig. 6). As the electrical response depends linearly on the charge concentration of the system, we can decompose σ_1 and σ_2 in two parts:

$$\sigma_i = \sigma^{\text{surf}} + \sigma_i^{\text{salt}}, \tag{3}$$

where σ^{surf} is the conductivity associated to the surfactant volume fraction, the same for both salt concentrations; σ_i^{salt} is the conductivity due only to the salt concentration in each case ($i = 1, 2$). If we take the difference $|\sigma_1 - \sigma_2|$, σ^{surf} is eliminated in Eq. (3) and we have a conductivity equivalent to that of a sponge phase swollen with a brine solution of salt concentration $|c_1 - c_2|$:

$$\sigma_{\text{eq}} = |\sigma_1 - \sigma_2| = \left|\sigma_1^{\text{salt}} - \sigma_2^{\text{salt}}\right|. \tag{4}$$

In our experiments, $c_1 = 100$ mM and $c_2 = 40$ mM, thus when we take the difference, the effective conductivity is that of a sponge phase swollen with a 60 mM brine solution, and we can compare it with the previously described non-ionic case.

As expected, the electrical conductivity of the TTAB–hexanol–brine sponge phase increases with the bilayer volume fraction, for both salt concentrations 40 and 100 mM. To obtain the obstruction factor f we must replace σ in Eq. (2) by $|\sigma_1 - \sigma_2|$; σ_0 must be the conductivity of a 60 mM brine solution. In Fig. 5 we also show f obtained by this procedure for the ionic sponge phase (squares). We see a remarkably linear behavior as expected for a sponge structure, similar to that observed in the non-ionic case. The extrapolation into $\phi \to 0$ gives a value smaller than 0.6. We also see that for all surfactant volume fractions, the obstruction factor of the ionic system is smaller than that of the non-ionic one. These facts are probably due to electrostatic interactions between the conducting ions and the charged bilayers. Note that the electrical conductivity results (Fig. 5) are an indication that the sponge phases are of symmetric topology, in agreement with the SAXS and FFEM experiments. The conductivity of asymmetric phases should be smaller due to the entrapment of ions inside the vesicles.

4. Conclusions

In this paper we report experiments on the sponge phases of the mixed system C_{14}DMAO–TTAB–hexanol–brine. We have extended a previous study of Hoffmann et al. [7] and showed that these phases can be stable in concentrated systems and at all proportions of ionic and non-ionic surfactants.

The SAXS, FFEM, and electrical conductivity experiments show that, for the same bilayer volume fraction, the sponge phases preserve the same global structure and have a symmetric topology. The only difference arises from the screened electrostatic interaction which gives rise to a bilayer thickness increasing with the ionic surfactant concentration. We proposed a method to obtain the geometrical obstruction factor f of ionic sponge phases from electrical conductivity measurements. The obtained f values are smaller for the ionic system, as compared with the non-ionic one, due to electrostatic interactions in the former.

The system characterized in this work can be used to test molecular effects arising from a variable charge density in the same lyotropic structure.

Acknowledgments

The authors thank the financial support from ECOS and ANUIES (action MOOP03). A.M. thanks financial support from the Consejo Nacional de Ciencia y Tecnología-Mexico (Grant 489100-5-J 32105E).

References

[1] W.M. Gelbart, A. Ben-Shaul, D. Roux (Eds.), Micelles, Membranes, Microemulsions and Monolayers, Springer-Verlag, 1994.
[2] B. Balinov, U. Olsson, O. Söderman, J. Phys. Chem. 95 (1991) 5931.
[3] R. Strey, R. Shomäcker, D. Roux, F. Nallet, U. Olsson, J. Chem. Soc. Faraday Trans. 86 (12) (1990) 2253.
[4] G. Porte, J. Marignan, P. Bassereau, R. May, J. Phys. (France) 49 (1988) 511.
[5] C.A. Miller, M. Gradzielski, H. Hoffmann, U. Krämer, C. Thunig, Colloid Polym. Sci. 268 (1990) 1066.
[6] C.G. Vonk, J.F. Billman, E.W. Kaler, J. Chem. Phys. 88 (6) (1988) 3970.
[7] G. Porte, J. Appell, P. Bassereau, J. Marignan, M. Skouri, I. Billard, M. Delsanti, Physica A 176 (1991) 168.
[8] J. Engblom, S.T. Hyde, J. Phys. II (France) 5 (1995) 171.
[9] I.S. Barnes, P.-J. Derian, S.T. Hyde, B.W. Ninham, T.N. Zemb, J. Phys. (France) 51 (1990) 2605.
[10] O. Abillon, B.P. Binks, D. Langevin, J. Meunier, Prog. Colloid Polym. Sci. 76 (1988) 84.

[11] A. Maldonado, W. Urbach, R. Ober, D. Langevin, Phys. Rev. E 54 (2) (1996) 1774.
[12] H. Hoffmann, U. Munkert, C. Thunig, M. Valiente, J. Colloid Interface Sci. 163 (1994) 217.
[13] D. Roux, C. Coulon, M.E. Cates, J. Phys. Chem. 96 (1992) 4174.
[14] M. Skouri, J. Marignan, J. Appell, G. Porte, J. Phys. II (France) 1 (1991) 1121.
[15] D. Gazeau, A.M. Bellocq, D. Roux, T. Zemb, Europhys. Lett. 9 (5) (1989) 447.
[16] T.N. Zemb, Colloids Surf. A Physicochem. Eng. Aspects 129–130 (1997) 435.